Dual-Spacecraft Formation Flying in Deep Space: Optimal Collision-Free Reconfigurations

Yoonsoo Kim* and Mehran Mesbahi†
University of Washington, Seattle, Washington 98195-2400
and
Fred Y. Hadaegh‡
Jet Propulsion Laboratory, California Institute of Technology, Pasadena, California 91109-8099

I. Introduction

THE distributed space system architecture has been identified as a new paradigm for many of the future NASA (Earth and deep space), U.S. Air Force, U.S. Navy, and commercial satellite space missions. Examples where the distributed space system technology will have a tremendous impact in the conceptualization and the development of the future space missions include space-borne optical interferometry, three-dimensional stereo imaging, robotic planetary explorations, and atmospheric monitoring and control.[1] At the same time, the distributed spacecraft framework poses a unique set of challenges in the areas of planning, guidance, and spacecraft control.[2–5] The most intuitive issues are in fact in the area of planning: For example, how a multiple spacecraft system should reconfigure itself while avoiding spacecraft collisions, a problem that is absent in the single spacecraft case. In this general venue, much effort has recently been devoted to devising conflict resolution algorithms for collision-free reconfigurations of multiple ground and aerial vehicles. These studies adopt a variety of approaches including game theory,[6] semidefinite programming,[7] potential fields,[8] and mixed-integer linear programming.[9] In this paper, we consider the optimal collision-free reconfiguration for a dual-spacecraft system as a state constrained optimal control problem.[10–15] It is often the case that such a problem formulation and the ensuing necessary optimality conditions do not lead to efficiently computable optimal control forces. However, we provide a solution to the dual-spacecraft optimal collision-free reconfiguration by relying on this approach.

The organization of the paper is as follows: In Sec. II, the mathematical formulation of the optimal collision-free dual spacecraft reconfiguration is presented. This is then followed by the characterization and the reparameterization of the optimal state trajectories and control forces via an optimal control formalism. Simulation results in Sec. III highlight some of the key features of the proposed framework for the dual-spacecraft reconfiguration problems.

II. Problem Statement and Parameterization of the Optimal Control

The problem considered in this paper is as follows: The initial inertial positions and the desired terminal relative position of the two spacecraft are given. We would like to specify the control forces that steer the dual spacecraft to the given terminal relative position, avoiding any collisions and requiring the minimum energy. We note that the desired inertial positions for the two spacecraft are not necessary specified. In other words, the dual spacecraft is allowed to assume an inertial terminal position that is consistent with the specified relative terminal position. Moreover, the path that each spacecraft has to traverse to achieve the required reconfiguration is not explicitly sought for, that is, the problem considered is not a guidance problem. Let us proceed now by denoting the translational inertial states of the two spacecraft i and j as x_i and x_j. Furthermore, let the respective control forces on the dual spacecraft be u_i and u_j. The optimal collision-free reconfiguration problem can thereby be stated as

$$J := \int_{t_0}^{t_f} u_i(t)^T u_i(t) + u_j(t)^T u_j(t)\,\mathrm{d}t \to \min \tag{1}$$

subject to the dynamic constraints,

$$\dot{x}_i(t) = Ax_i(t) + B_i u_i(t), \qquad \dot{x}_j(t) = Ax_j(t) + B_j u_j(t) \tag{2}$$

initial inertial and final relative positions, $x_i(t_0)$, $x_j(t_0)$, and $x_i(t_f) - x_j(t_f)$, and for the parameter $\rho_{ij} > 0$, the collision avoidance constraint,

$$\|C\{x_i(t) - x_j(t)\}\| \geq \rho_{ij}, \qquad \text{for all} \qquad t \in [t_0, t_f] \tag{3}$$

where $\|.\|$ denotes the 2-norm. In Eq. (2) and (3), one has $A \in \boldsymbol{R}^{6\times 6}$, $B_i, B_j \in \boldsymbol{R}^{6\times 3}$, and $C \in \boldsymbol{R}^{3\times 6}$, where

$$A = \begin{bmatrix} 0_{3\times 3} & I_{3\times 3} \\ 0_{3\times 3} & 0_{3\times 3} \end{bmatrix}, \qquad B_i = \frac{1}{m_i}\begin{bmatrix} 0_{3\times 3} \\ I_{3\times 3} \end{bmatrix}$$

$$B_j = \frac{1}{m_j}\begin{bmatrix} 0_{3\times 3} \\ I_{3\times 3} \end{bmatrix}, \qquad C = [I_{3\times 3} \quad 0_{3\times 3}]$$

and m_i and m_j denote the mass of spacecraft i and j, respectively. We note that a double integrator has been employed to represent each spacecraft dynamics, effectively ignoring the orbital forces. This simplification has been adopted in view of the following observation. Consider a deep space Earth-trailing dual-spacecraft formation flying mission, with its two spacecraft only a few kilometers apart. Assume furthermore that the masses of the two spacecraft are on the order of a few hundred kilograms. Then when the linearized Hill's equation (see Ref. 16) is used, it can be shown that the differential orbital force between the two spacecraft is on the order of 10^{-23} N. Because the reconfiguration scenarios that we are interested in occur on relatively short timescales (as compared to, for example, 365 days), ignoring the differential orbital forces in this work is well justified.

Let us first reparameterize the optimal control problem Eqs. (1–3) in terms of the relative state of the two spacecraft $z(t) := x_i(t) - x_j(t) \in \boldsymbol{R}^6$. With the combined control force u defined as $u(t) := [u_i(t)\ u_j(t)]^T \in \boldsymbol{R}^6$, the reparameterization optimal control problem takes the form

$$J := \int_{t_0}^{t_f} u(t)^T u(t)\,\mathrm{d}t \to \min \tag{4}$$

subject to the dynamics

$$\dot{z}(t) = Az(t) + Bu(t) \tag{5}$$

relative initial and desired terminal states $z(t_0)$ and $z(t_f)$ and the relative state constraint

$$z(t)^T C^T C z(t) \geq \rho_{ij}^2, \qquad \text{for all} \qquad t \in [t_0, t_f] \tag{6}$$

In this case one has

$$A = \begin{bmatrix} 0_{3\times 3} & I_{3\times 3} \\ 0_{3\times 3} & 0_{3\times 3} \end{bmatrix}, \qquad B = \begin{bmatrix} 0_{3\times 3} & 0_{3\times 3} \\ (1/m_i)I_{3\times 3} & (-1/m_j)I_{3\times 3} \end{bmatrix}$$

$$C = [I_{3\times 3} \quad 0_{3\times 3}] \tag{7}$$

Let us point out several characteristics of the optimal dual-spacecraft reconfiguration problem as represented by Eqs. (4–6). First, we note

Received 27 July 2001; revision received 22 September 2002; accepted for publication 25 October 2002.

*Graduate Student, Department of Aeronautics and Astronautics, Box 352400; yoonsoo@aa.washington.edu.

†Assistant Professor, Department of Aeronautics and Astronautics, Box 352400; mesbahi@aa.washington.edu.

‡Senior Research Scientist, Autonomy and Control Section, 4800 Oak Grove Drive, Mail Stop 198-326; fred.y.hadaegh@jpl.nasa.gov. Associate Fellow AIAA.

that the dynamics of the two spacecraft are merely coupled through the final desired relative position and the pointwise-in-time state constraints Eq. (6). The diameter of the collision avoidance region ρ_{ij} in Eq. (6), in general, is a reflection of the designer's assessment of how far the actual spacecraft is away from being a point mass. Moreover, given that we envision the dual-spacecraft reconfiguration to be an integral part of a timed space mission, the final time t_f has been specified in the objective functional Eq. (4). The most distinguishing feature of the optimal control problem Eqs. (4–6) is the presence of the state inequality constraint as expressed by Eq. (6). The presence of this constraint complicates the form of the necessary optimality conditions; moreover, it makes the process of guessing the form of the optimal solution, and then checking whether it satisfies the necessary conditions, much more challenging. Thus, we proceed to approach this problem by considering two separate modes, corresponding the active/inactive condition of the inequality constraint Eq. (6). We note that, at the outset, it is not clear when this transition, from constrained to unconstrained mode, and vice versa, takes place for the optimal control forces. In the absence of any other reasonable guess on the switching times, we assume that the unconstrained mode corresponds to $[U] = [U_1] \cup [U_2]$, where $[U_1] := [t_0, t_1]$ and $[U_2] := [t_2, t_f]$, and the constrained mode corresponds to $[C] := [t_0, t_f] \backslash [U] = [t_1, t_2]$; with this assumption intact, we now proceed to derive the mode-dependent necessary optimality conditions.

First, consider the Hamiltonian $\mathcal{H} := u(t)^T u(t) + \lambda(t)^T \{Az(t) + Bu(t)\}$ and the Lagrangian $\mathcal{L} := \mathcal{H} + \mu(t)\{z(t)^T C^T C z(t) - \rho_{ij}^2\}$ functionals for the optimal control problem Eqs. (4–6), where $\lambda(t)$ and $\mu(t)$ are the multipliers that adjoin the constraints expressed by Eqs. (5) and (6), respectively. When the inequality state constraint Eq. (6) is inactive, that is, $z(t)^T C^T C z(t) > \rho_{ij}^2$, the multiplier $\mu(t)$ is set to zero. In this case, the Lagrangian reduces to the Hamiltonian recovering the classical, state constrained-free, optimal energy control problem. The necessary optimality conditions for the unconstrained mode are[12]

$$\dot{\lambda}(t)^T = -\lambda(t)^T A, \qquad \dot{z}(t) = Az(t) + Bu(t)$$
$$0 = 2u(t)^T + \lambda(t)^T B \tag{8}$$

with the vectors $z(t_0)$ and $z(t_f)$ already specified. From Eq. (8), it now follows that the optimal state and control trajectories during the first unconstrained mode assume the forms

$$z(t)^{[U_1]} = m \begin{bmatrix} (1/6)(t-t_0)^2(t+2t_0) I_{3\times 3} & (-1/2)(t-t_0)^2 I_{3\times 3} \\ (1/2)(t-t_0)(t+t_0) I_{3\times 3} & -(t-t_0) I_{3\times 3} \end{bmatrix} \boldsymbol{y}^{[U_1]} + \begin{bmatrix} z_1(t_0) + (t-t_0) z_2(t_0) \\ z_2(t_0) \end{bmatrix} \tag{9}$$

$$u(t)^{[U_1]} = \frac{1}{2} \begin{bmatrix} (t/m_i) I_{3\times 3} & (-1/m_i) I_{3\times 3} \\ (-t/m_j) I_{3\times 3} & (1/m_j) I_{3\times 3} \end{bmatrix} \boldsymbol{y}^{[U_1]} \tag{10}$$

where $m = (m_i^2 + m_j^2)/(2m_i^2 m_j^2)$. Similarly, for the second unconstrained mode, one has

$$z(t)^{[U_2]} = m \begin{bmatrix} (1/6)(t-t_f)^2(t+2t_f) I_{3\times 3} & (-1/2)(t-t_f)^2 I_{3\times 3} \\ (1/2)(t-t_f)(t+t_f) I_{3\times 3} & -(t-t_f) I_{3\times 3} \end{bmatrix} \boldsymbol{y}^{[U_2]} + \begin{bmatrix} z_1(t_f) + (t-t_f) z_2(t_f) \\ z_2(t_f) \end{bmatrix} \tag{11}$$

$$u(t)^{[U_2]} = \frac{1}{2} \begin{bmatrix} (t/m_i) I_{3\times 3} & (-1/m_i) I_{3\times 3} \\ (-t/m_j) I_{3\times 3} & (1/m_j) I_{3\times 3} \end{bmatrix} \boldsymbol{y}^{[U_2]} \tag{12}$$

The yet unspecified vectors $\boldsymbol{y}^{[U_1]}, \boldsymbol{y}^{[U_2]} \in \boldsymbol{R}^6$ in Eqs. (9–12) will be determined shortly via the boundary conditions. For the constrained mode, corresponding to the time interval $[t_1, t_2]$, we let $z(t)^T C^T C z(t) = \rho_{ij}^2$. In this case, the necessary optimality conditions are[12,13]

$$\dot{\lambda}(t)^T = -\lambda(t)^T A - 2\mu(t) z(t)^T C^T C, \qquad 0 = 2u(t)^T + \lambda(t)^T B$$
$$\dot{z}(t) = Az(t) + Bu(t), \qquad z(t)^T C^T C z(t) = \rho_{ij}^2 \tag{13}$$

The expressions for the state trajectories and control forces that satisfy the necessary conditions Eq. (13) can be derived explicitly as[1]

$$z(t)^{[C]} = \begin{bmatrix} \rho_{ij} \cos(\omega t + \phi_1) \cos\phi_2 \\ \rho_{ij} \cos(\omega t + \phi_1) \sin\phi_2 \\ \rho_{ij} \sin(\omega t + \phi_1) \\ -\rho_{ij}\omega \sin(\omega t + \phi_1) \cos\phi_2 \\ -\rho_{ij}\omega \sin(\omega t + \phi_1) \sin\phi_2 \\ \rho_{ij}\omega \cos(\omega t + \phi_1) \end{bmatrix}$$

$$u(t)^{[C]} = \frac{\rho_{ij}\omega^2}{2m} \begin{bmatrix} -(1/m_i) \cos(\omega t + \phi_1) \cos\phi_2 \\ -(1/m_i) \cos(\omega t + \phi_1) \sin\phi_2 \\ -(1/m_i) \sin(\omega t + \phi_1) \\ (1/m_j) \cos(\omega t + \phi_1) \cos\phi_2 \\ (1/m_j) \cos(\omega t + \phi_1) \sin\phi_2 \\ (1/m_j) \sin(\omega t + \phi_1) \end{bmatrix} \tag{14}$$

The yet unspecified parameters ω, ϕ_1, and ϕ_2, will also be determined shortly. We note that a state feedback form of the optimal control forces in Eqs. (10), (12), and (14) can also be obtained for the unconstrained and constrained modes (see earlier web address).

We now consider the issues pertaining to the switching between the unconstrained and the constrained operational modes for the optimal dual-spacecraft reconfiguration. In this venue, we have already characterized the forms of the optimal state and control trajectories in each of mode, separately. Therefore, we need to further specify 1) the time interval $[t_1, t_2]$ corresponding to the mode switching in and out of the constrained mode and 2) the parameters ω, ϕ_1, and ϕ_2 that determine when and for how long the relative state of the two spacecraft lives on the constrained region. We proceed to address both issues using a continuity argument and a parameter minimization procedure. We first note that because the relative state $z(t)$ is continuously differentiable, its continuity, in conjunction with the knowledge of the initial and terminal conditions, $z(t_0)$ and $z(t_f)$, can be employed to express the vectors $\boldsymbol{y}^{[U_1]}$ and $\boldsymbol{y}^{[U_2]}$ in Eqs. (9) and (11), as a function of the parameters t_1, t_2, ω, ϕ_1, and ϕ_2. This is accomplished by enforcing the boundary conditions $z(t_1)^{[U_1]} = z(t_1)^{[C]}$ and $z(t_2)^{[C]} = z(t_2)^{[U_2]}$. By substituting these expressions in Eqs. (9–12), we obtain a parameterization of the optimal control forces and, thus, the objective functional J Eq. (4) in terms of the parameters t_1, t_2, ω, ϕ_1, and ϕ_2. Furthermore, when $t_2 = \alpha t_1$ is set, for $\alpha \geq 1$, this parameterization assumes the form of $J(t_1, \omega, \phi_1, \phi_2, \alpha)$. The exact functional form of this expression for J turns out to be

$$J(t_1, \omega, \phi_1, \phi_2, \alpha) = (\alpha - 1) t_1 \rho_{ij}^2 \omega^4 \big/ 2 + A \big/ (t_1 - t_0)^3 + B \big/ (\alpha t_1 - t_f)^3 \tag{15}$$

where

$$A = 6\rho_{ij}^2 + 2(t_1 - t_0)^2 \rho_{ij}^2 \omega^2 + 6\|z_1(t_0)\|^2 + 6(t_1 - t_0) z_{11}(t_0) z_{21}(t_0) + 2(t_1 - t_0)^2 z_{21}(t_0)^2 + 6(t_1 - t_0) z_{12}(t_0) z_{22}(t_0) + 2(t_1 - t_0)^2 z_{22}(t_0)^2 + 2(t_1 - t_0)^2 z_{23}(t_0)^2 + 6(t_1 - t_0) z_{13}(t_0) z_{23}(t_0) + 2(t_1 - t_0)\rho_{ij}\omega\{3z_{13}(t_0) + (t_1 - t_0) z_{23}(t_0)\} \cos(\phi_1 + t_1\omega) - \rho_{ij}\{6z_{11}(t_0) + (t_1 - t_0)[3(\omega + 1) z_{21}(t_0) + (t_1 - t_0)\omega z_{22}(t_0)]\} \times \cos(\phi_1 - \phi_2 + t_1\omega) + \rho_{ij}\{-6z_{11}(t_0) - 3(t_1 - t_0) z_{21}(t_0)$$

$$+3(t_1-t_0)\omega z_{12}(t_0)+(t_1-t_0)^2\omega z_{22}(t_0)\big\}\cos(\phi_1+\phi_2+t_1\omega)$$
$$-6\rho_{ij}\{2z_{13}(t_0)+(t_1-t_0)z_{23}(t_0)\}\sin(\phi_1+t_1\omega)$$
$$+\rho_{ij}\big\{-3(t_1-t_0)\omega z_{11}(t_0)-(t_1-t_0)^2\omega z_{21}(t_0)$$
$$+3(t_1-t_0)z_{22}(t_0)+6z_{12}(t_0)\big\}\sin(\phi_1-\phi_2+t_1\omega)$$
$$-\rho_{ij}\big\{\big[3(t_1-t_0)\omega z_{11}(t_0)+(t_1-t_0)^2\omega z_{21}(t_0)+6z_{12}(t_0)$$
$$+3(t_1-t_0)z_{22}(t_0)\big]\big\}\times\sin(\phi_1+\phi_2+t_1\omega)$$

$$B=-6\rho_{ij}^2-2(\alpha t_1-t_f)^2\rho_{ij}^2\omega^2-6\|z_1(t_f)\|^2$$
$$-6(\alpha t_1-t_f)z_{11}(t_f)z_{21}(t_f)-2(\alpha t_1-t_f)^2z_{21}(t_f)^2$$
$$-6(\alpha t_1-t_f)z_{12}(t_f)z_{22}(t_f)-2(\alpha t_1-t_f)^2z_{22}(t_f)^2$$
$$-6(\alpha t_1-t_f)z_{13}(t_f)z_{23}(t_f)-2(\alpha t_1-t_f)^2z_{23}(t_f)^2$$
$$-2(\alpha t_1-t_f)\rho_{ij}\omega\times\{3z_{13}(t_f)+(\alpha t_1-t_f)z_{23}(t_f)\}$$
$$\times\cos(\phi_1+\alpha t_1\omega)+\rho_{ij}\{6z_{11}(t_f)+(\alpha t_1-t_f)$$
$$\times[3(\omega+1)z_{12}(t_f)+(\alpha t_1-t_f)\omega z_{22}(t_f)]\}$$
$$\times\cos(\phi_1-\phi_2+\alpha t_1\omega)+\rho_{ij}\big\{6z_{11}(t_f)$$
$$+3(\alpha t_1-t_f)[z_{21}(t_f)-\omega z_{12}(t_f)]-(\alpha t_1-t_f)^2\omega z_{22}(t_f)\big\}$$
$$\times\cos(\phi_1+\phi_2+\alpha t_1\omega)+6\rho_{ij}\{2z_{13}(t_f)+(\alpha t_1-t_f)z_{23}(t_f)\}$$
$$\times\sin(\phi_1+\alpha t_1\omega)+\rho_{ij}\big\{3(\alpha t_1-t_f)\omega z_{11}(t_f)$$
$$+(\alpha t_1-t_f)^2\omega z_{21}(t_f)-6z_{12}(t_f)-3(\alpha t_1-t_f)\times z_{22}(t_f)\big\}$$
$$\times\sin(\phi_1-\phi_2+\alpha t_1\omega)+\rho_{ij}\big\{3(\alpha t_1-t_f)\omega z_{11}(t_f)$$
$$+(\alpha t_1-t_f)^2\omega\times z_{21}(t_f)+6z_{12}(t_f)+3(\alpha t_1-t_f)z_{22}(t_f)\big\}$$
$$\times\sin(\phi_1+\phi_2+\alpha t_1\omega)$$

Here $z_1(t)=[z_{11}(t)\ \ z_{12}(t)\ \ z_{13}(t)]^T$ and $z_2(t)=[z_{21}(t)\ \ z_{22}(t)\ \ z_{23}(t)]^T$. When this parameterization is used, it can shown that the performance index J is a nondecreasing function of α. Thus, a judicious strategy is to choose the parameter α as close to one as possible. In this direction, suppose that we initiate the procedure for finding the optimal control forces and the optimal state trajectories by fixing α. The objective functional thus assumes the form $J_\alpha(t_1,\omega,\phi_1,\phi_2):=J(t_1,\omega,\phi_1,\phi_2,\alpha)$. Consider then finding the minimizers of J_α, denoted by $t_1^*(\alpha)$, $\omega^*(\alpha)$, $\phi_1^*(\alpha)$, and $\phi_2^*(\alpha)$. Having found these minimizing parameters, one can then proceed to construct the corresponding candidate optimal relative state trajectory $z_\alpha^*(t)$ and the optimal control forces $u_\alpha^*(t)$. The quintuple $\{\alpha, t_1^*(\alpha), \omega^*(\alpha), \phi_1^*(\alpha), \phi_2^*(\alpha)\}$, however, may or may not lead to a feasible state trajectory, depending on our choice of the parameter α. (Note that we are carefully avoiding having to solve a constrained nonconvex optimization problem.) Our proposed procedure thereby involves a search subroutine for the value of α that leads to a feasible as well as an optimal relative state trajectory. The complete procedure is summarized as follows: 1) Given the initial and desired terminal relative configurations, parameterize the objective functional J Eq. (4) via the parameters t_1, ω, ϕ_1, ϕ_2, and α in Eq. (15). This is accomplished by using the continuity conditions at t_1 and t_2 to eliminate the vectors $\mathbf{y}^{[U_i]}$, $i=1,2$, in Eqs. (9–11), and finally by letting $t_2=\alpha t_1$. 2) Let us assume that, without loss of generality, $t_0>0$; then because $\alpha t_1=t_2\le t_f$ and $t_1\ge t_0$, we conclude that $\alpha\le t_f/t_0$. Now for a fixed value of $1\le\alpha\le t_f/t_0$, solve the system of nonlinear equations $\nabla J_\alpha(t_1,\omega,\phi_1,\phi_2)=0$ for the minimizing parameters t_1^*, ω^*, ϕ_1^*, and ϕ_2^*, leading to the candidate optimal state trajectory and optimal control forces. 3) If this constructed relative state trajectory is feasible, the control forces obtained are in fact optimal, and we terminate the procedure. Otherwise, a line search procedure is utilized, keeping in mind that the constrained region should not be traversed more than halfway, until a feasible relative state trajectory is found.

We conclude this section by commenting on an intuitive result pertaining to the relationship between the optimal performance Eq. (4) and the diameter of the constraint region ρ_{ij} Eq. (6). In fact, it can be shown that during the constrained mode, one has $\partial J^*/\partial\rho_{ij}^2=-\mu(t)=2\omega^4/m$, where $m=(m_i^2+m_j^2)/(2m_i^2m_j^2)$. Because the multiplier $\mu(t)$ is set to zero during the unconstrained mode, the rather intuitive relation $\partial J^*/\partial\rho_{ij}^2\ge 0$ now follows directly: The optimal performance is a nondecreasing function of the diameter of the collision avoidance region.

III. Simulation Results

We illustrate the viability of the proposed algorithm through two representative dual-spacecraft reconfiguration scenarios: case A, where $x_1(0)=[0\ 0\ 0\ 0\ 0\ 0]^T$, $x_2(0)=[10\ 10\ 10\ 0\ 0\ 0]^T$, and $x_1(10)-x_2(10)=[10\ 10\ 10\ 0\ 0\ 0]^T$; and case B, where $x_1(0)=[4.5\ 0\ 0\ 0.5\ 0\ 0]^T$, $x_2(0)=[8\ 0\ 0\ 0\ 0\ 0]^T$, and $x_1(10)-x_2(10)=[3.5\ 0\ 0\ 0\ 0\ 0]^T$. For both cases, the terminal time is set to 10 time units ρ_{ij}, the required minimum relative distance is set to three length units, and the mass of each spacecraft is set to one mass unit. For case A, the initial and desired final states are such that the two spacecraft are required to interchange their positions; we note that they are not a priori required to attain particular inertial positions. When $\alpha=1$, the optimal control forces are obtained by solving the four equations $\partial J_\alpha/\partial t_1=0$, $\partial J_\alpha/\partial\omega=0$, $\partial J_\alpha/\partial\phi_1=0$, and $\partial J_\alpha/\partial\phi_2=0$, for the minimizing parameters t_1^*, ω^*, ϕ_1^*, and ϕ_2^*, and subsequently substituting these values into Eqs. (10), (12), and (14). These values are found to be $t_1^*=5.0000$, $\omega^*=-1.7304$, $\phi_1^*=-1.7281$, and $\phi_2^*=\pi/4=0.7854$. Figure 1 shows the corresponding optimal state trajectory. We note that each spacecraft does in fact attain the initial inertial position of the other. Moreover, for case A, it turns out that the value $\alpha=1$, that is, $t_1=t_2$, leads to a feasible relative state trajectory. Figure 2 confirms that a feasible state trajectory is obtained by setting $\alpha=1$ and that the relative state trajectory contacts the constraint region at $t=5$.

For case B, we chose the initial and the terminal desired relative positions such that the dual spacecraft is close to violating the constraint at both instances. In fact, we note that one of the spacecraft has an initial velocity that is pointing toward the constrained region. For this case the value of the parameter α that leads to a feasible trajectory turns out to be strictly greater than one, that is, $t_1\ne t_2$. This is in view of the fact that after calculating t_1^*, ω^*, ϕ_1^*, and ϕ_2^* for $\alpha=1$, the candidate optimal relative state trajectory is not feasible. Thus, we proceeded to search for a suitable value of α as prescribed in Sec. II. In this venue, we determined that, when $\alpha=3.19$, the resulting relative state trajectory traverses the boundary during the time interval $[C]=[2.1347, 6.8097]$. Figures 3 and 4 show several state trajectories of the dual-spacecraft system for various choices of the parameter α. As the parameter α increases toward the value

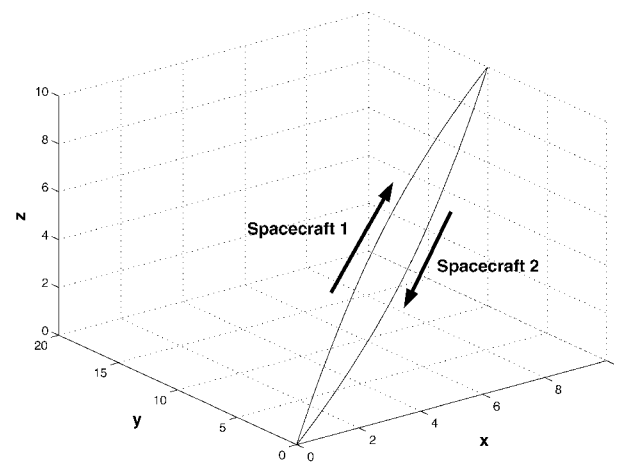

Fig. 1 Optimal spacecraft trajectories for case A.

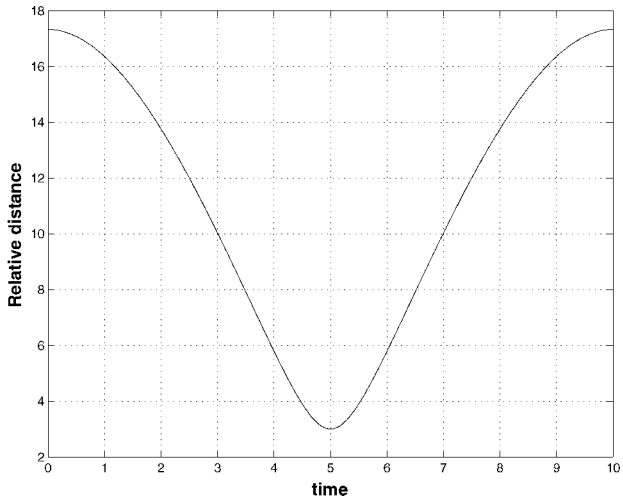

Fig. 2 Relative distance between the two spacecraft for case A.

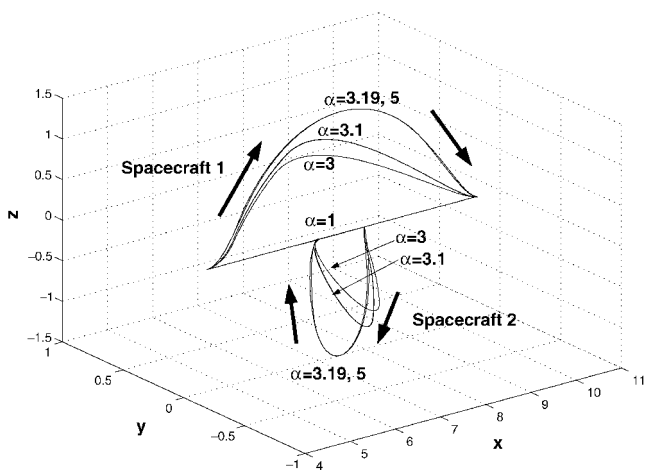

Fig. 3 Optimal spacecraft trajectories for case B.

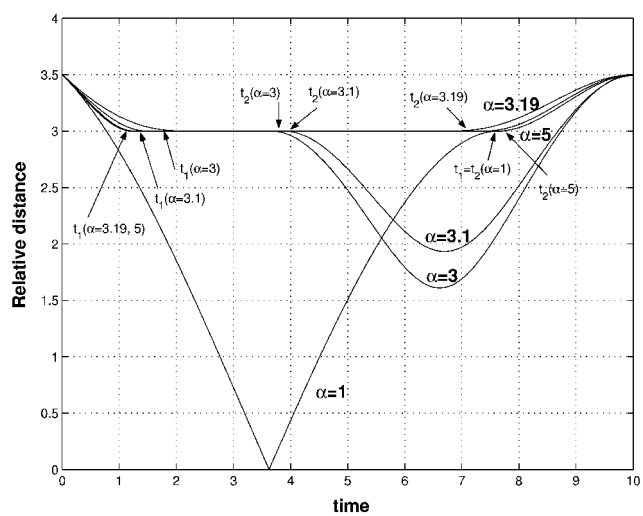

Fig. 4 Relative distance between the two spacecraft for case B.

3.19 (Fig. 4), a feasible and optimal trajectory is realized. Figures 3 and 4 also show that, for parameter value $\alpha = 5 > 3.19$, the corresponding state trajectory remains feasible; however, it now traverses the constrained mode for a longer time period. Figure 5 shows the optimal control forces for case B when $\alpha = 3.19$. As in the earlier case, the solid and the dashed lines represent, respectively, the first and the second spacecraft optimal control forces. We note that the control forces associated with the two unconstrained modes $u^{[U_1]}$ and $u^{[U_2]}$ are linear, as they are for case A; this linear behavior, however, vanishes during the constrained mode $[C] = [2.1347, 6.8097]$. For case B, the values of the parameters ω^*, ϕ_1^*, ϕ_2^*, t_1^*, t_2^*, and J_α^* are tabulated for several values of α in Table 1.

Table 1 Parameter values for several choices of α for case B

α	ω^*	ϕ_1^*	ϕ_2^*	t_1^*	t_2^*	J_α^*
1.00	−0.0006	0.0053	0.0000	7.6378	7.6378	0.4139
3.10	−0.2608	3.2895	0.0000	1.2549	3.8902	1.1981
3.19	−0.3894	3.4619	0.0000	2.1347	6.8097	1.2197
3.50	−0.3873	3.4478	0.0000	1.9789	6.9262	1.2252
5.00	−0.3770	3.3865	0.0000	1.4811	7.4055	1.3017

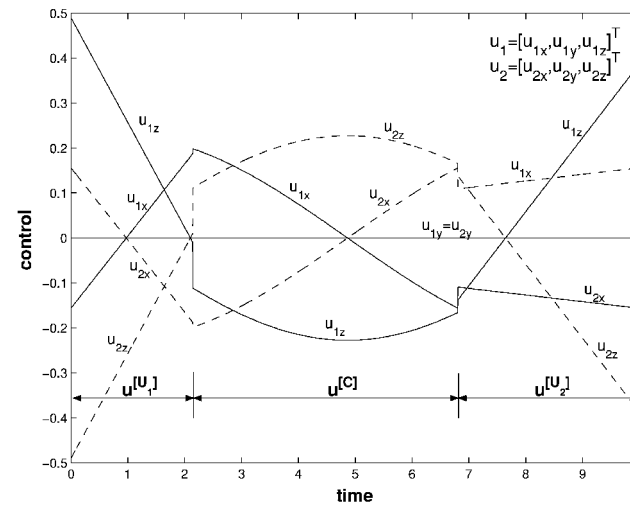

Fig. 5 Optimal control forces for case B.

IV. Concluding Remarks

We solved the deep space optimal dual-spacecraft reconfiguration problem in the presence of a collision avoidance requirement. Our approach is distinguished by its reliance on the necessary optimality conditions, similar in spirit to the Euler–Lagrange equations. In this venue, we identified the collision avoidance guarantee as a state inequality constraint in the corresponding optimal control problem. This modification significantly changes the solution characteristic of the optimal control and involves the introduction of the nonsmooth multiplier, which dynamically monitors the violation of the state constraints. The time evolution of this multiplier essentially determines the switching times, which in turn, lead to the characterization of the optimal relative state trajectory. At the same time, we recognize that the extension of the proposed approach to more than two spacecraft scenarios involves expressions for the control parameters that are not easy to solve. However, the proposed scheme can be employed to obtain nontrivial upper bounds for the general optimal multiple spacecraft reconfiguration by reducing it to a sequence of two-at-a-time collision-free reconfigurations.

Acknowledgments

The research of Y. Kim and M. Mesbahi was supported by National Science Foundation grant CMS-0093456 and by a grant from Jet Propulsion Laboratory, California Institute of Technology, under a contract with NASA. The research of F. Y. Hadaegh was carried out at the Jet Propulsion Laboratory, California Institute of Technology, under a contract with NASA. The authors thank Y. Zhao from the University of Minnesota and the anonymous reviewers for helpful comments and suggestions during the preparation of the manuscript.

Reference

[1] "Terrestrial Planet Finder: Origins of Stars, Planets, and Life," Jet Propulsion Lab., California Inst. of Technology, Pasadena, CA, May 1999.

[2] Wang, P. K. C., and Hadaegh, F. Y., "Coordination and Control of Multiple Microspacecraft Moving in Formation," *Journal of the Astronautical Sciences*, Vol. 44, No. 3, 1996, pp. 315–355.

[3]Beard, R., Lawton, J., and Hadaegh, F. Y., "A Coordination Architecture for Spacecraft Formation Control," *IEEE Transactions on Control Systems Technology*, Vol. 9, No. 6, 2001, pp. 777–790.

[4]Kang, W., Sparks, A., and Banda, S., "Coordinated Control of Multisatellite Systems," *Journal of Guidance, Control, and Dynamics*, Vol. 24, No. 2, 2001, pp. 360–368.

[5]Mesbahi, M., and Hadaegh, F. Y., "Formation Flying Control of Multiple Spacecraft via Graphs, Matrix Inequalities, and Switching," *Journal of Guidance, Control, and Dynamics*, Vol. 24, No. 2, 2001, pp. 369–377.

[6]Tomlin, C., Pappas, G. J., and Sastry, S., "Noncooperative Conflict Resolution," *IEEE Conference on Decision and Control*, IEEE Publications, Piscataway, NJ, 1997, pp. 1816–1821.

[7]Frazzoli, E., Mao, Z. H., Oh, J. H., and Feron, E., "Aircraft Conflict Resolution via Semidefinite Programming," *Journal of Guidance, Control, and Dynamics*, Vol. 24, No. 1, 2001, pp. 79–86.

[8]Ghosh, R., and Tomlin, C., "Maneuver Design for Multiple Aircraft Conflict Resolution," *American Control Conference*, American Automatic Control Council, Evanston, IL, 2000, pp. 28–30.

[9]Richards, A., Schouwenaars, T., How, J., and Feron, E., "Spacecraft Trajectory Planning with Collision and Plum Avoidance Using Mixed-Integer Linear Programming," *Journal of Guidance, Control, and Dynamics*, Vol. 25, No. 4, 2002, pp. 755–765.

[10]Gregory, J., and Lin, C., *Constrained Optimization in the Calculus of Variations and Optimal Control Theory*, Springer-Verlag, New York, 1992, pp. 83–128.

[11]Mehra, R. K., and Davis, R. E., "A Generalized Gradient Method for Optimal Control Problems with Inequality Constraints and Singular Arcs," *IEEE Transactions on Automatic Control*, Vol. 17, No. 1, 1972, pp. 69–78.

[12]Stengel, R. F., *Optimal Control and Estimation*, Dover, New York, 1994.

[13]Vinter, R., *Optimal Control*, Birkhaüser, Boston, 2000, pp. 321–360.

[14]Bryson, A., Denham, W., and Dreyfus, S., "Optimal Programming Problems with Inequality Constraints, Part 1: Necessary Conditions for Extremal Solutions," *AIAA Journal*, Vol. 1, No. 11, 1963, pp. 2544–2550.

[15]Speyer, J., and Bryson, A., "Optimal Programming Problems with a Bounded State Space," *AIAA Journal*, Vol. 6, No. 8, 1968, pp. 1488–1491.

[16]Sidi, M., *Spacecraft Dynamics and Control*, Cambridge Univ. Press, Cambridge, England, U.K., 1997.